Active Fractional-Order Sliding Mode Control of Flexible Spacecraft Under Actuators Saturation

milad alipour
University of Isfahan
Maryam Malekzadeh (m.malekzadeh@eng.ui.ac.ir)
University of Isfahan Faculty of Engineering https://orcid.org/0000-0003-1922-4488
alireza ariaei
University of Isfahan Faculty of Engineering

Research Article

Keywords: Flexible Spacecraft, Fractional-Order Nonsingular Terminal Sliding Mode (FONTSM), Active Vibration Suppression, Actuators Saturation, Fixed-Time Stability

Posted Date: April 5th, 2021

DOI: https://doi.org/10.21203/rs.3.rs-331089/v1

Noname manuscript No.
(will be inserted by the editor)

Active Fractional-Order Sliding Mode Control of Flexible Spacecraft Under Actuators Saturation

Milad Alipour · Maryam Malekzadeh · Alireza Ariaei

Received: date / Accepted: date

Abstract In this article, a novel multi-purpose modified fractional-order nonsingular terminal sliding mode (MFONTSM) controller is designed for the flexible spacecraft attitude control, assuming the control torque saturation in the system dynamics. The proposed controller is modified to be able to perform appendages passive vibration suppression. Furthermore, an active FONTSM controller is proposed separately to perform active vibration suppression of the flexible appendages using piezoelectric actuators. The closed-loop system's fixed-time stability for both the passive and active controllers is analyzed and proved using the Lyapunov theorem. Finally, the proposed controllers' performance has been tested in the presence of uncertainties, external disturbances, and the absence of the damping matrix in order to study the effectiveness of the proposed method.

Keywords Flexible Spacecraft · Fractional-Order Nonsingular Terminal Sliding Mode (FONTSM) · Active Vibration Suppression · Actuators Saturation · Fixed-Time Stability

Milad Alipour
Department of Mechanical Engineering, University of Isfahan, Iran
E-mail: m.alipour@eng.ui.ac.ir

Maryam Malekzadeh
Department of Mechanical Engineering, University of Isfahan, Iran
Tel.: +98-31-37934111
Fax: +98-31-37932746
E-mail: m.malekzadeh@eng.ui.ac.ir

Alireza Ariaei
Department of Mechanical Engineering, University of Isfahan, Iran
Tel.: +98-31-37934054
Fax: +98-31-37932746
E-mail: ariaei@eng.ui.ac.ir

1 Introduction

The emergence of new missions that usually require high-pointing accuracy, along with uncertainties and external disturbances, make the precise attitude control of spacecraft vital for mission accomplishment. Furthermore, cost reduction often requires the modern spacecraft to have large and lightweight, flexible appendages, which results in increased structural flexibility. Therefore, the problem of flexible spacecraft attitude control with appendages vibration suppression becomes more crucial and challenging than before.

In the past decades, for the flexible spacecraft vibration suppression, some active control methods have been suggested, such as component synthesis vibration suppression (CSVS) [1], modal velocity feedback compensator (MVFC) [2, 3], strain rate feedback compensator (SRFC) [3], and positive position feedback (PPF) [4, 5]. However, they usually concentrate on the attitude controller's innovation rather than the active controller [6]. Besides, most of them usually ignore the coupling term in the modal equation from the beginning of the attitude maneuver, despite its effect on the elastic mode vibrations. Hence, a desired active controller must either consider this term or be robust against its effects; otherwise, the system's stability is not fully guaranteed. Some passive vibration suppression methods usually consider flexible influences as external disturbance [7]. Although the above approaches can effectively reduce the appendages' vibrations, they rely solely on the attitude controller to reduce elastic vibrations' influence on the spacecraft attitude. In other words, the vibration itself is not suppressed but rather decayed through the damping of the structures. However, when the structures have low damping and high

flexibility, these methods may not maintain the desired results.

In reality, since practical actuators' control output is always limited regardless of their type, the actuators' saturation, often as a dominant input nonlinearity, may severely limit the system performance and even lead to instability or undesirable inaccuracy. Thus far, various control schemes considering actuators saturation have been proposed. For instance, in [8], a tangent hyperbolic function and in [9, 10] a saturation function was used in systems dynamics to describe actuators saturation. Then, [10] has been further studied by [11], and it was observed that the method was ineffective. Another approach is to augment a new equation, representing the actuators saturation, to the system dynamics [12]. However, this method results in prolonged settling time, reducing the practicality of the control approach. The majority of research on spacecraft attitude control generally ignores the actuators' saturation problem despite its inevitable effect on attitude maneuvers. Moreover, there is minimal research on attitude control design and stability analysis with explicit consideration of the flexible spacecraft's actuators' saturation.

In recent years, the 300-year-old fractional calculus concept has been combined with terminal sliding mode (TSM) and nonsingular terminal sliding mode (NTSM) methods. The resulting controllers have all the advantages of the NTSM controller with better transient performance and faster convergence due to the freedom on the integrator and differentiator order. These novel controllers have been used for various systems, including robot manipulator [13], cable-driven manipulator [14], and linear motor [15]. Nevertheless, in some of these works, the error signals' stability and boundedness after reaching the sliding surface are not mathematically studied. In the others with a complete stability analysis, the control law usually consists of a fractional-order differentiator. Unlike the fractional-order integrator, the fractional-order differentiator's boundedness is not studied; thus, the control law's boundedness is not fully guaranteed.

Moreover, as mentioned so far, most of the research provides finite-time stability for the system where the exact upper bound of the settling time depends on the initial conditions. Therefore, to address this issue, the concept of fixed-time stability was introduced [16]. According to this concept, the settling time function is upper bounded by a predefined constant that depends on the design parameters rather than the system's initial state [17]. Consequently, the convergence time can be designed in a prescribed manner.

In this work, we propose two novel controllers for the flexible spacecraft's attitude control and vibration suppression to address the problems mentioned above. The main contributions of this paper are as follows:

(i) A novel multi-purpose MFONTSM controller is designed to perform fast attitude stabilization and provide passive vibration suppression, considering the actuators' saturation in the system's dynamics. Furthermore, a new active FONTSM controller is introduced to perform active vibration suppression using the piezoelectric actuators.

(ii) The closed-loop system's practical fixed-time stability under external disturbance, uncertainty, and actuators' saturation is analyzed and proved using the Lyapunov theorem. The proposed control method's effectiveness has been studied through comparative numerical simulations under the damping matrix's absence.

The rest of the paper is organized in the following manner: In Section 2, some preliminaries of the concepts of fractional calculus and fixed-time stability are given. Section 3 denotes the problem statement. In Section 4, the controller design and stability analysis are presented. The comparative numerical simulations are represented in Section 5, and Section 6 concludes the paper.

2 Preliminaries

The three most commonly used definitions of fractional calculus are Riemann-Liouville (RL) definition, Grünwald-Letnikov (GL) definition, and Caputo (C) definition [18].

Definition 1 [18] The RL definition:

$$ {}^{RL}_{t_0}\mathrm{D}^{\alpha}_{t}\, f(t) = \frac{1}{\Gamma(n-\alpha)} \left(\frac{d}{dt}\right)^{n} \int_{t_0}^{t} \frac{f(\tau)}{(t-\tau)^{\alpha-n+1}} d\tau $$

where α is the fractional order.

Definition 2 [18] The GL definition:

$$ {}^{GL}_{t_0}\mathrm{D}^{\alpha}_{t}\, f(t) = \lim_{h\to 0} \frac{1}{h^{\alpha}} \sum_{j=0}^{\lfloor (t-t_0)/h \rfloor} (-1)^{j} \binom{\alpha}{j} f(t-jh) $$

where h is the sampling interval, and $\lfloor x \rfloor, \quad x \in R$ is a flooring operator which gives the integer part of its input, also,

$$ \binom{\alpha}{j} = \frac{\Gamma(\alpha+1)}{\Gamma(j+1)\Gamma(\alpha-j+1)} $$

where $\Gamma(x) = \int_0^{\infty} e^{-t} t^{x-1}\, dt$ is the well-known Gamma function.

Property 1 [19] Let $\alpha > 0$, $n = \lceil \alpha \rceil$, $f(t) \in C^n[a,b]$, then

$$ {}^{GL}\mathrm{D}^{\alpha} f(t) = {}^{RL}\mathrm{D}^{\alpha} f(t), \qquad \forall t \in (a,b] $$

Property 2 [19] Let $\alpha > 0$, $f \in C[a,b]$, then

$$ {}^{GL}\mathrm{D}^{-\alpha} f(t) = {}^{RL}\mathrm{D}^{-\alpha} f(t), \qquad \forall t \in [a,b] $$

Lemma 1 *[20] Fractional integration operator* ${}_{t_0}\mathrm{D}_t^{-\alpha}$, $(t > t_0,\ \alpha \in C,\ \Re(\alpha) > 0)$ *is bounded in* $L_p(\hat{a},\hat{b})$, $(1 \le p \le \infty,\ -\infty < \hat{a} < \hat{b} < \infty)$*:*

$$ \| {}_{t_0}\mathrm{D}_t^{-\alpha} f(t)\|_p \le \kappa \|f(t)\|_p, \quad \left(\kappa = \frac{(\hat{b}-\hat{a})^{\Re(\alpha)}}{\Re(\alpha)|\Gamma(\alpha)|}\right) $$

Lemma 2 *[10, 21] Consider a nonlinear system*

$$ \dot{x}(t) = f(x(t)), \quad x(0) = 0, \quad f(0) = 0, \quad x \in R^n \qquad (1) $$

where $f : U_0 \to R^n$ *is continuous in an open neighborhood* U_0 *of the origin, the unique solution of (1) is supposed to exist for any initial conditions. The nonlinear system (1) is practical fixed-time stable in case that there exists a Lyapunov function* $V(x)$*, scalars* $a, b \in R^+$, $0 < a < 1$, $b > 1$, $\alpha > 0$, $\beta > 0$ *and* $0 \le \vartheta < \infty$ *such that* $\dot{V}(x) \le -\alpha V(x)^a - \beta V(x)^b + \vartheta$ *holds. Therefore, the trajectory of the closed-loop system is bounded in fixed-time as*

$$ \lim_{t \to T} x \mid V(x) \le \min\left\{ \left(\frac{\vartheta}{(1-\theta)\alpha}\right)^{\frac{1}{a}}, \left(\frac{\vartheta}{(1-\theta)\beta}\right)^{\frac{1}{b}} \right\} $$

where θ *is scalar and satisfies* $0 < \theta \le 1$*. The time to reach the residual set i.e. the settling time* T *is bounded by*

$$ T \le T_{max} \triangleq \frac{1}{\alpha}\frac{1}{1-a} + \frac{1}{\beta}\frac{1}{b-1} $$

Remark 1 The GL definition is commonly used to describe practical cases because of its clear expression and simplicity of implementation. As seen from Property 1 and 2, for a wide class of functions, important for the application, both RL and GL definitions are equivalent. Therefore, the RL definition can be used during problem formulation and then turn to GL definition for obtaining the numerical solutions [18]. Consequently, in this paper, a finite approximation of GL definition based on Power Series Expansion (PSE) of a generating function with $h = 10^{-3}$ has been used for implementation [22]. Furthermore, for the purpose of simplicity we use D^{α} instead of ${}_{t_0}\mathrm{D}_t^{\alpha}$, for the rest of this paper.

Fig. 1: Schematic of the flexible spacecraft

3 Problem Statement

3.1 Attitude Kinematics and Dynamics

As shown in Fig. 1, the simplified flexible spacecraft consists of a rigid hub and two flexible appendages.

Assuming that the thin, homogeneous, and isotropic piezoelectric films are attached on the surface of the flexible appendages as actuators; the attitude kinematic and dynamic model of the flexible spacecraft is given as [1]:

$$ \begin{cases} \dot{q}_0 = -\frac{1}{2}\mathbf{q}^T\boldsymbol{\omega} \\ \dot{\mathbf{q}} = \frac{1}{2}(q_0\mathbf{I} + \mathbf{q}^{\times})\boldsymbol{\omega} \end{cases} \qquad (2) $$

$$ \mathbf{J}\dot{\boldsymbol{\omega}} + \boldsymbol{\delta}^T\ddot{\boldsymbol{\eta}} + \boldsymbol{\omega}^{\times}(\mathbf{J}\boldsymbol{\omega} + \dot{\boldsymbol{\eta}}) = \mathbf{u} + \mathbf{d} \qquad (3) $$

$$ \ddot{\boldsymbol{\eta}} + \mathbf{C}\dot{\boldsymbol{\eta}} + \mathbf{K}\boldsymbol{\eta} + \boldsymbol{\delta}\dot{\boldsymbol{\omega}} = -\boldsymbol{\delta}_p\mathbf{u}_p \qquad (4) $$

Equation (2) is the kinematic equation, where $[q_0,\ \mathbf{q}]^T = [q_0,\ q_1,\ q_2,\ q_3]^T \in R^4$ is the quaternion representation of the body frame attitude orientation with respect to an inertial frame, $q_0 \in R$ and $\mathbf{q} = [q_1,\ q_2,\ q_3]^T \in R^3$ are scalar and vector components of the unit quaternion, respectively, and $\mathbf{q}^T\mathbf{q} + q_0^2 = 1$. Also, $\mathbf{I} \in R^{3\times 3}$ is the identity matrix, and $\boldsymbol{\omega} \in R^3$ denotes the angular velocity of the spacecraft expressed in the body frame relative to the inertial frame. Equation (3) is the attitude dynamic equation, where $\mathbf{J} \in R^{3\times 3}$ is the positive definite symmetric inertia matrix of the spacecraft, $\mathbf{u} \in R^3$ and $\mathbf{d} \in R^3$ represent the control torque and external disturbance torque acting on the spacecraft, respectively. $\boldsymbol{\delta} \in R^{3\times n}$ denotes the coupling matrix between the rigid hub and flexible appendages, and $\boldsymbol{\eta} \in R^n$ represents the $n-$dimensional modal displacement. Equation (4) is the modal equation, where $\boldsymbol{\delta}_p \in R^{n\times m}$ is a coupling matrix associated with the structural characteristics of the

appendage and the mounting position of the n piezoelectric sensors and m piezoelectric actuators. $\mathbf{u}_p \in R^m$ denotes the $m-$dimensional piezoelectric input voltage. $\mathbf{C} = 2\boldsymbol{\zeta}\boldsymbol{\Omega} \in R^{n\times n}$ and $\mathbf{K} = \boldsymbol{\Omega}^2 \in R^{n\times n}$ are the diagonal damping and stiffness matrices, respectively, where $\boldsymbol{\zeta} \in R^{n\times n}$ and $\boldsymbol{\Omega} \in R^{n\times n}$ represent the flexible appendages diagonal matrices of damping ratio and natural frequency, respectively. The notation $\mathbf{x}^\times \in R^{3\times 3}$ represents the cross-product matrix operator of an arbitrary vector $\mathbf{x} = [x_1,\, x_2,\, x_3]^T \in R^3$ defined by:

$$\mathbf{x}^\times = \begin{bmatrix} 0 & -x_3 & x_2 \\ x_3 & 0 & -x_1 \\ -x_2 & x_1 & 0 \end{bmatrix}$$

3.2 Relative Attitude Error

Assuming $\boldsymbol{\varphi} = [\phi,\, \theta,\, \psi]^T$ describes the rotation angles of the spacecraft body frame axes with respect to the inertial frame. Let $\boldsymbol{\varphi}_d = [\phi_d,\, \theta_d,\, \psi_d]^T$ represent the desired rotation angles and $[q_{d0},\, \mathbf{q}_d]^T$, $\mathbf{q}_d \in R^3$, $q_{d0} \in R$ the desired quaternion parameters, respectively. Using the standard coordinate transformation, one can reformulate the attitude tracking problem into a stabilization problem as [23]:

$$\begin{cases} q_{e0} = \mathbf{q}_d^T\mathbf{q} + q_{d0}q_0 \\ \mathbf{q}_e = q_{d0}\mathbf{q} - \mathbf{q}_d^\times\mathbf{q} - q_0\mathbf{q}_d \\ \boldsymbol{\omega}_e = \boldsymbol{\omega} - \mathbf{R}\boldsymbol{\omega}_d \end{cases} \tag{5}$$

where $q_{e0} \in R$ and $\mathbf{q}_e \in R^3$ denote the error quaternion, $\boldsymbol{\omega}_d \in R^3$ is the desired angular velocity with respect to the inertial frame expressed in the reference body frame, $\boldsymbol{\omega}_e$ denotes the relative angular velocity error and the matrix $\mathbf{R} = (1 - 2\mathbf{q}_e^T\mathbf{q}_e)\mathbf{I} + 2\mathbf{q}_e\mathbf{q}_e^T - 2q_{e0}\mathbf{q}_e^\times$ is the rotation matrix with the conditions $\|\mathbf{R}\| = 1$ and $\dot{\mathbf{R}} = -\boldsymbol{\omega}_e^\times\mathbf{R}$ in which $\|\mathbf{x}\|$ represents the L_2 norm of a vector or matrix. Substituting (4) in (3) and considering $\dot{\boldsymbol{\omega}} = \dot{\boldsymbol{\omega}}_e + \boldsymbol{\omega}_e^\times\mathbf{R}\boldsymbol{\omega}_d - \mathbf{R}\dot{\boldsymbol{\omega}}_d$, the relative attitude error equations can be obtained as

$$\begin{cases} \dot{q}_{e0} = -\frac{1}{2}\mathbf{q}_e^T\boldsymbol{\omega}_e \\ \dot{\mathbf{q}}_e = \frac{1}{2}(q_e\mathbf{I} + \mathbf{q}_e^\times)\boldsymbol{\omega}_e \end{cases} \tag{6}$$

$$\mathbf{J}_0\dot{\boldsymbol{\omega}}_e = -\boldsymbol{\omega}^\times\mathbf{J}(\boldsymbol{\omega} + \boldsymbol{\delta}^T\dot{\boldsymbol{\eta}}) + \boldsymbol{\delta}^T(\mathbf{C}\dot{\boldsymbol{\eta}} + \mathbf{K}\boldsymbol{\eta} + \boldsymbol{\delta}_p\mathbf{u}_p) + \mathbf{J}_0(\boldsymbol{\omega}_e^\times\mathbf{R}\boldsymbol{\omega}_d - \mathbf{R}\dot{\boldsymbol{\omega}}_d) + \mathbf{u} + \mathbf{d} \tag{7}$$

where $\mathbf{J}_0 = \mathbf{J} - \boldsymbol{\delta}^T\boldsymbol{\delta}$, and the term $\boldsymbol{\delta}^T\boldsymbol{\delta}$ is the effect of the flexible appendages on the total inertia matrix.

4 Controller Design and Stability Analysis

This section presents the main results regarding the controller design and stability analysis of the system.

4.1 Attitude Controller Design

A FONTSM sliding surface can be proposed as $\mathbf{s} = \dot{\mathbf{q}}_e + \boldsymbol{\Lambda}\,\mathrm{D}^{\alpha-2}[\mathrm{sig}(\mathbf{q}_e)^\lambda]$, that can only provide attitude control but no passive vibration suppression. Now by modifying the given sliding surface we propose our modified FONTSM or MFONTSM sliding surface $\mathbf{s}_1 \in R^3$ as

$$\mathbf{s}_1 = \dot{\mathbf{q}}_e + \boldsymbol{\Lambda}\,\mathrm{D}^{\alpha-2}[\mathrm{sig}(\mathbf{q}_e)^\lambda] + \boldsymbol{\Delta}_1\,\mathrm{D}^{\beta_1-2}[\mathrm{sig}(\dot{\boldsymbol{\eta}}_e)^{\delta_1}] + \boldsymbol{\Delta}_2\,\mathrm{D}^{\beta_2-2}[\mathrm{sig}(\boldsymbol{\eta}_e)^{\delta_2}] \tag{8}$$

where $\boldsymbol{\eta}_e = \boldsymbol{\eta}_d - \boldsymbol{\eta}$ and $\dot{\boldsymbol{\eta}}_e = \dot{\boldsymbol{\eta}}_d - \dot{\boldsymbol{\eta}}$ are the appendages modal displacement error and modal velocity error, respectively. $\boldsymbol{\Lambda} = \mathrm{diag}(\Lambda_1, \Lambda_2, \Lambda_3)$, $\boldsymbol{\Delta}_1 = \mathrm{diag}(\Delta_{11}, \Delta_{12}, \Delta_{13})$ and $\boldsymbol{\Delta}_2 = \mathrm{diag}(\Delta_{21}, \Delta_{22}, \Delta_{23})$ are positive constant diagonal matrices. α, β_1 and β_2 are fractional-orders which $0 < \alpha, \beta_1, \beta_2 < 1$. Furthermore, λ, δ_1 and δ_2 are terminal fractions satisfying $0 < \lambda, \delta_1, \delta_2 < 1$. For an arbitrary vector $\mathbf{x} = [x_1,\, x_2,\, x_3]^T$ and the scalar ζ, the notation $\mathrm{sig}(\mathbf{x})^\zeta$ denotes:

$$\mathrm{sig}(\mathbf{x})^\zeta = [|x_1|^\zeta\,\mathrm{sgn}(x_1),\, |x_2|^\zeta\,\mathrm{sgn}(x_2),\, |x_3|^\zeta\,\mathrm{sgn}(x_3)]^T$$

where $\mathrm{sgn}(x)$ stands for the signum function.

Remark 2 The sliding surface given in most of the existing literature on FONTSM controllers, for example [13,14], can be written as

$$\bar{\mathbf{s}} = \dot{\tilde{\mathbf{q}}} + \boldsymbol{\Lambda}\,\mathrm{D}^{\alpha-1}[\mathrm{sig}(\tilde{\mathbf{q}})^\lambda] \tag{9}$$

where $\tilde{\mathbf{q}}$ represents the error states of the system and the other parameters for (9) are similar to that of (8). The single-purpose sliding surface (9) is a one-variable fractional-order equation that is only able to bring the error states on the sliding surface. Meanwhile, our multi-purpose sliding surface (8) represents a multi-variable fractional-order equation that can bring the error quaternion, modal velocity error, and modal displacement error on the sliding surface at the same time. Furthermore, the term $\mathrm{D}^{\alpha-1}$ in (9) is a fractional integrator which according to Lemma 1 is bounded. However, calculating the first derivative of (9) will result in the appearance of the term D^α in the control input, which is a fractional differentiator, and therefore, the boundedness of the control input is not fully guaranteed. This problem has been solved with our proposed sliding surface.

Calculating the first derivative of (8), we obtain

$$\dot{\mathbf{s}}_1 = \ddot{\mathbf{q}}_e + \boldsymbol{\Lambda}\,\mathrm{D}^{\alpha-1}[\mathrm{sig}(\mathbf{q}_e)^\lambda] + \boldsymbol{\Delta}_1\,\mathrm{D}^{\beta_1-1}[\mathrm{sig}(\dot{\boldsymbol{\eta}}_e)^{\delta_1}] + \boldsymbol{\Delta}_2\,\mathrm{D}^{\beta_2-1}[\mathrm{sig}(\boldsymbol{\eta}_e)^{\delta_2}] \tag{10}$$

Calculating the derivative of (6) yields:

$$\ddot{\mathbf{q}}_e = \frac{1}{2}(\dot{q}_{e0}\mathbf{I} + \dot{\mathbf{q}}_e^{\times})\boldsymbol{\omega}_e + \frac{1}{2}(q_{e0}\mathbf{I} + \mathbf{q}_e^{\times})\dot{\boldsymbol{\omega}}_e \tag{11}$$

Using (7) and (5) we can obtain $\ddot{\mathbf{q}}_e$ as:

$$\begin{aligned}\ddot{\mathbf{q}}_e &= \frac{1}{2}(\dot{q}_{e0}\mathbf{I} + \dot{\mathbf{q}}_e^{\times})\boldsymbol{\omega}_e \\ &+\frac{1}{2}(q_{e0}\mathbf{I}+\mathbf{q}_e^{\times})\mathbf{J}_0^{-1}\big(-\boldsymbol{\omega}^{\times}\mathbf{J}(\boldsymbol{\omega}+\boldsymbol{\delta}^T\dot{\boldsymbol{\eta}})+\boldsymbol{\delta}^T(\mathbf{C}\dot{\boldsymbol{\eta}}+\mathbf{K}\boldsymbol{\eta}+\boldsymbol{\delta}_p\mathbf{u}_p) \\ &\quad + \mathbf{J}_0(\boldsymbol{\omega}_e^{\times}\mathbf{R}\boldsymbol{\omega}_d - \mathbf{R}\dot{\boldsymbol{\omega}}_d) + \mathbf{u} + \mathbf{d}\big)\end{aligned} \tag{12}$$

Substituting (12) in (10) we can simply obtain:

$$\begin{aligned}\dot{\mathbf{s}}_1 &= \frac{1}{2}(\dot{q}_{e0}\mathbf{I} + \dot{\mathbf{q}}_e^{\times})\boldsymbol{\omega}_e \\ &+\frac{1}{2}(q_{e0}\mathbf{I}+\mathbf{q}_e^{\times})\mathbf{J}_0^{-1}\big(-\boldsymbol{\omega}^{\times}\mathbf{J}(\boldsymbol{\omega}+\boldsymbol{\delta}^T\dot{\boldsymbol{\eta}})+\boldsymbol{\delta}^T(\mathbf{C}\dot{\boldsymbol{\eta}}+\mathbf{K}\boldsymbol{\eta}+\boldsymbol{\delta}_p\mathbf{u}_p) \\ &+ \mathbf{J}_0(\boldsymbol{\omega}_e^{\times}\mathbf{R}\boldsymbol{\omega}_d - \mathbf{R}\dot{\boldsymbol{\omega}}_d) + \mathbf{u} + \mathbf{d}\big) + \boldsymbol{\Lambda}\,\mathrm{D}^{\alpha-1}[\mathrm{sig}(\mathbf{q}_e)^{\lambda}] \\ &\quad + \boldsymbol{\Delta}_1\,\mathrm{D}^{\beta_1-1}[\mathrm{sig}(\dot{\boldsymbol{\eta}}_e)^{\delta_1}] + \boldsymbol{\Delta}_2\,\mathrm{D}^{\beta_2-1}[\mathrm{sig}(\boldsymbol{\eta}_e)^{\delta_2}]\end{aligned} \tag{13}$$

To obtain a precise and fast control performance invariant to initial conditions, we propose a fixed-time fast TSM type reaching law as:

$$\dot{\mathbf{s}}_1 = -\mathbf{K}_1\,\mathrm{sig}(\mathbf{s}_1)^m - \mathbf{K}_2\,\mathrm{sig}(\mathbf{s}_1)^n \tag{14}$$

where the matrices $\mathbf{K}_1 = \mathrm{diag}(K_{11}, K_{12}, K_{13})$ and $\mathbf{K}_2 = \mathrm{diag}(K_{21}, K_{22}, K_{23})$ are constant diagonal positive matrices to be designed. m and n are positive integers which $0 < m < 1$ and $n > 1$.

Remark 3 The reaching law in the aforementioned papers can be written as

$$\dot{\bar{\mathbf{s}}} = -\mathbf{K}_1\,\mathrm{sig}(\bar{\mathbf{s}})^m - \mathbf{K}_2\bar{\mathbf{s}} \tag{15}$$

where all the parameters for (15) are similar to that of (14). Compared to (14), the reaching law (15) can only provide finite-time stability for the closed-loop system which heavily relies on the initial conditions.

Now we can find the control input with substituting (14) in (13) and neglecting the disturbance term. Therefore, we obtain:

$$\mathbf{u} = -\mathbf{G}^{-1}\big(\mathbf{f} + \mathbf{K}_1\,\mathrm{sig}(\mathbf{s}_1)^m + \mathbf{K}_2\,\mathrm{sig}(\mathbf{s}_1)^n\big) \tag{16}$$

where $\mathbf{G}$ and $\mathbf{f}$ are:

$$\mathbf{G} = \frac{1}{2}(q_{e0}\mathbf{I} + \mathbf{q}_e^{\times})\mathbf{J}_0^{-1}$$

$$\begin{aligned}\mathbf{f} &= \frac{1}{2}(\dot{q}_{e0}\mathbf{I} + \dot{\mathbf{q}}_e^{\times})\boldsymbol{\omega}_e \\ &+ \mathbf{G}\big(-\boldsymbol{\omega}^{\times}\mathbf{J}(\boldsymbol{\omega} + \boldsymbol{\delta}^T\dot{\boldsymbol{\eta}}) + \boldsymbol{\delta}^T(\mathbf{C}\dot{\boldsymbol{\eta}} + \mathbf{K}\boldsymbol{\eta} + \boldsymbol{\delta}_p\mathbf{u}_p) \\ &+ \mathbf{J}_0(\boldsymbol{\omega}_e^{\times}\mathbf{R}\boldsymbol{\omega}_d - \mathbf{R}\dot{\boldsymbol{\omega}}_d)\big) + \boldsymbol{\Lambda}\,\mathrm{D}^{\alpha-1}[\mathrm{sig}(\mathbf{q}_e)^{\lambda}] \\ &\quad + \boldsymbol{\Delta}_1\,\mathrm{D}^{\beta_1-1}[\mathrm{sig}(\dot{\boldsymbol{\eta}}_e)^{\delta_1}] + \boldsymbol{\Delta}_2\,\mathrm{D}^{\beta_2-1}[\mathrm{sig}(\boldsymbol{\eta}_e)^{\delta_2}]\end{aligned}$$

Remark 4 If we set $\boldsymbol{\Delta}_1 = \boldsymbol{\Delta}_2 = \mathbf{0}$ in the sliding surface (8) and the controller (16), we get FONTSM sliding surface and controller. Therefore, for the purpose of comparison, we will study both FONTSM and MFONTSM controllers.

4.2 Actuators Saturation

In this section, we redesign the attitude controller to consider the actuators' saturation bound. The dynamic equation of the flexible spacecraft with actuators saturation can be expressed as [24]:

$$\mathbf{J}\dot{\boldsymbol{\omega}} + \boldsymbol{\delta}^T\ddot{\boldsymbol{\eta}} + \boldsymbol{\omega}^{\times}(\mathbf{J}\boldsymbol{\omega} + \dot{\boldsymbol{\eta}}) = \mathrm{sat}(\mathbf{u}) + \mathbf{d} \tag{17}$$

Similarly the error dynamic equation is derived as:

$$\begin{aligned}\mathbf{J}_0\dot{\boldsymbol{\omega}}_e = &-\boldsymbol{\omega}^{\times}\mathbf{J}(\boldsymbol{\omega} + \boldsymbol{\delta}^T\dot{\boldsymbol{\eta}}) + \boldsymbol{\delta}^T(\mathbf{C}\dot{\boldsymbol{\eta}} + \mathbf{K}\boldsymbol{\eta} + \boldsymbol{\delta}_p\mathbf{u}_p) \\ &+ \mathbf{J}_0(\boldsymbol{\omega}_e^{\times}\mathbf{R}\boldsymbol{\omega}_d - \mathbf{R}\dot{\boldsymbol{\omega}}_d) + \mathrm{sat}(\mathbf{u}) + \mathbf{d}\end{aligned} \tag{18}$$

where the saturation function $\mathrm{sat}(\mathbf{u})$ is defined as:

$$\mathrm{sat}(\mathbf{u}) = \mathrm{sgn}(\mathbf{u})\min\{|\mathbf{u}|, \mathbf{u}_{max}\} \tag{19}$$

where we have $\mathbf{u}_{max} = u_{max}[1\ 1\ 1]^T$, and u_{max} is the upper bound of the control torque saturation.

Now inspired by [25] we propose the saturated MFONTSM controller as:

$$\mathrm{sat}(\mathbf{u}) = \mathrm{sat}(\mathbf{z} - \mu\mathbf{s}_1) \tag{20}$$

where μ is a positive scalar and $\mathbf{z}$ is the same as the control law $\mathbf{u}$ defined in (16).

Equation (20) forms the proposed saturated MFONTSM attitude controller of this paper.

4.3 Active Vibration Controller Design

To proceed further, the following basic assumption is required in this section:

Assumption 1 *The number of the piezoelectric actuators and sensors is equal, and they are mounted in such a way that the coupling matrix $\boldsymbol{\delta}_p$ is invertible [6].*

Suppose that the attitude controller works in a way that the spacecraft reaches the desired attitude, in other words, as $t \to \infty$, then $q_{e0} \to 1$, $\mathbf{q}_e \to \mathbf{0}$, $\boldsymbol{\omega}_e \to \mathbf{0}$ and $\dot{\boldsymbol{\omega}}_e \to \mathbf{0}$, that results in the elastic motion to asymptotically decouple from the rigid one. In this case spacecraft attitude has been successfully controlled, however, the bounded elastic oscillation might still persist in the flexible panels. With defining $\mathbf{d}_p = \boldsymbol{\delta}\dot{\boldsymbol{\omega}}$ as an external disturbance acting on the flexible panels, (4) can be written as following

$$\ddot{\boldsymbol{\eta}} + \mathbf{C}\dot{\boldsymbol{\eta}} + \mathbf{K}\boldsymbol{\eta} = -\boldsymbol{\delta}_p\mathbf{u}_p - \mathbf{d}_p \tag{21}$$

Remark 5 In most of the research regarding the active controller design, for example, [2, 4], the controller is designed by setting $\dot{\boldsymbol{\omega}} = \mathbf{0}$ in the modal equation, which leads to a decoupled lower dynamics. Therefore, the effect of the term $\boldsymbol{\delta}\dot{\boldsymbol{\omega}}$ on the appendages' vibrations is ignored from the maneuver's beginning even though the angular velocity rate becomes zero only at the end of the attitude stabilization maneuvers.

Now similar to the attitude controller design, we need to design a proper sliding surface for the active vibration controller as well. Therefore, we propose a second sliding surface $\mathbf{s}_2 \in R^3$ as

$$\mathbf{s}_2 = \dot{\boldsymbol{\eta}} + \boldsymbol{\Gamma}_1 \, \mathrm{D}^{\rho_1 - 2}[\mathrm{sig}(\dot{\boldsymbol{\eta}})^{\gamma_1}] + \boldsymbol{\Gamma}_2 \, \mathrm{D}^{\rho_2 - 2}[\mathrm{sig}(\boldsymbol{\eta})^{\gamma_2}] \quad (22)$$

where $\boldsymbol{\Gamma}_1 = \mathrm{diag}(\Gamma_{11}, \Gamma_{12}, \Gamma_{13})$ and $\boldsymbol{\Gamma}_2 = \mathrm{diag}(\Gamma_{21}, \Gamma_{22}, \Gamma_{23})$ are positive constant diagonal matrices. ρ_1 and ρ_2 are fractional-orders which $0 < \rho_1, \rho_2 < 1$. Furthermore, γ_1 and γ_2 are terminal fractions satisfying $0 < \gamma_1, \gamma_2 < 1$. Calculating the first derivative of (22) and substituting (21) yields

$$\dot{\mathbf{s}}_2 = -(\mathbf{C}\dot{\boldsymbol{\eta}} + \mathbf{K}\boldsymbol{\eta} + \boldsymbol{\delta}_p \mathbf{u}_p + \mathbf{d}_p) + \boldsymbol{\Gamma}_1 \, \mathrm{D}^{\rho_1 - 1}[\mathrm{sig}(\dot{\boldsymbol{\eta}})^{\gamma_1}] + \boldsymbol{\Gamma}_2 \, \mathrm{D}^{\rho_2 - 1}[\mathrm{sig}(\boldsymbol{\eta})^{\gamma_2}] \quad (23)$$

Now similar to (14), a fixed-time fast TSM type reaching law is designed as:

$$\dot{\mathbf{s}}_2 = -\mathbf{L}_1 \, \mathrm{sig}(\mathbf{s}_2)^p - \mathbf{L}_2 \, \mathrm{sig}(\mathbf{s}_2)^r \quad (24)$$

where the matrices $\mathbf{L}_1 = \mathrm{diag}(L_{11}, L_{12}, L_{13})$ and $\mathbf{L}_2 = \mathrm{diag}(L_{21}, L_{22}, L_{23})$ are constant diagonal positive matrices to be designed. p and r are positive integers which $0 < p < 1$ and $r > 1$.

Now we can find the active control input with substituting (24) in (23). Thus, similar to (16), we obtain:

$$\mathbf{u}_p = -\mathbf{G}_p^{-1}\big(\mathbf{f}_p + \mathbf{L}_1 \, \mathrm{sig}(\mathbf{s}_2)^p + \mathbf{L}_2 \, \mathrm{sig}(\mathbf{s}_2)^r\big) \quad (25)$$

where $\mathbf{G}_p$ and $\mathbf{f}_p$ are:

$$\mathbf{G}_p = -\boldsymbol{\delta}_p$$

$$\mathbf{f}_p = -(\mathbf{C}\dot{\boldsymbol{\eta}} + \mathbf{K}\boldsymbol{\eta}) + \boldsymbol{\Gamma}_1 \, \mathrm{D}^{\rho_1 - 1}[\mathrm{sig}(\dot{\boldsymbol{\eta}})^{\gamma_1}] + \boldsymbol{\Gamma}_2 \, \mathrm{D}^{\rho_2 - 1}[\mathrm{sig}(\boldsymbol{\eta})^{\gamma_2}]$$

Equation (25) forms the proposed active vibration controller of this paper.

4.4 Stability Analysis

In order to start the stability analysis of the proposed controllers, we need the following assumptions.

Assumption 2 *The total disturbance* $\mathbf{d}$ *is bounded, but the upper bound is unknown:*

$$\|\mathbf{d}\| \leq d_{max}$$

Assumption 3 *The inertia matrix* $\mathbf{J}_0$ *with uncertainty is bounded, but the upper bound is unknown:*

$$\begin{aligned} \|\mathbf{J}_0\| &= \|\mathbf{J} - \boldsymbol{\delta}^T\boldsymbol{\delta}\| \\ &\leq \|\mathbf{J}\| + \|\boldsymbol{\delta}^T\boldsymbol{\delta}\| \\ &\leq \|\mathbf{J}\| + \|\boldsymbol{\delta}^T\|\|\boldsymbol{\delta}\| \\ &\leq J_{max} + \delta_{max}^2 \triangleq J_{0max} \end{aligned}$$

Assumption 4 *The matrix* $\mathbf{G}$ *in (16) is bounded and invertible:*

Considering Assumption 3 since the matrix $\mathbf{J}_0$ *is bounded we can deduce that,* $\mathbf{J}_0^{-1}$ *is bounded as well, therefore:*

$$\|\mathbf{J}_0^{-1}\| \leq \bar{J}_{0max}$$

and for the matrix $(q_{e0}\mathbf{I} + \mathbf{q}_e^{\times})$ *we have [23]:*

$$\|(q_{e0}\mathbf{I} + \mathbf{q}_e^{\times})\| \leq 1$$

we can calculate the bound of $\mathbf{G}$ *as:*

$$\begin{aligned} \|\mathbf{G}\| &= \frac{1}{2}\|(q_{e0}\mathbf{I} + \mathbf{q}_e^{\times})\mathbf{J}_0^{-1}\| \\ &\leq \frac{1}{2}\|(q_{e0}\mathbf{I} + \mathbf{q}_e^{\times})\|\|\mathbf{J}_0^{-1}\| \\ &\leq \frac{1}{2}\bar{J}_{0max} \end{aligned}$$

thus, the matrix $\mathbf{G}$ *is bounded as well. To ensure* $\mathbf{G}$ *is invertible, the matrix* $(q_{e0}\mathbf{I} + \mathbf{q}_e^{\times})$ *should be invertible as well. In other words [26]:*

$$\det(q_{e0}\mathbf{I} + \mathbf{q}_e^{\times}) = q_{e0} \neq 0, \qquad \forall t \in [0, \infty) \quad (26)$$

to ensure (26) remains valid, attitude maneuver should be restricted that $q_{e0}(0) \neq 0$*, where* $q_{e0}(0)$ *represents the initial conditions of* q_{e0}*, and the subsequent control strategies should be designed to guarantee that* $q_{e0} \neq 0$ *for all time. Therefore, in this study, for the matrix* $\mathbf{G}$ *to be invertible and to avoid quaternion singularity, we limit the range of the attitude maneuver to* $(+\pi, -\pi)$*.*

Theorem 1 *For the spacecraft attitude control and modal vibration systems in (2), (3) and (4), with the proposed sliding surface in (8) and the designed attitude controller with actuators saturation in (20), if the Assumptions 1, 2, 3 and 4 hold, the sliding surface of the attitude controller will reach a small neighborhood of origin within a fixed time, and all the corresponding signals of the closed-loop system will converge to a small neighborhood of origin in finite time, in the presence of unknown external disturbance and uncertainty.*

Proof There are two main steps in this proof. Step 1 shows the sliding surface $\mathbf{s}_1$, will reach in a small neighborhood of origin within a fixed time and proves the practical fixed-time stability of the system. Step 2 ensures that, once the trajectory of the closed-loop system is driven onto the sliding surface, then $\mathbf{q}_e$, $\dot{\mathbf{q}}_e$, $\dot{\boldsymbol{\eta}}_e$ and $\boldsymbol{\eta}_e$ of the closed-loop system will remain bounded thereafter.

Step 1 *The saturation function (20) can be rewritten as*

$$\mathrm{sat}(\mathbf{u}) = \mathrm{sat}(\mathbf{z} - \mu\mathbf{s}_1) = \mathbf{z} - [\mathrm{sat}(\mu\mathbf{s}_1 - \mathbf{z}) + \mathbf{z}] \tag{27}$$

where

$$\mathrm{sat}(\mu\mathbf{s}_1 - \mathbf{z}) + \mathbf{z} = \begin{cases} \mathbf{z} + \mathbf{u}_{max}, & if\ (\mu\mathbf{s}_1 - \mathbf{z}) > \mathbf{u}_{max} \\ \mu\mathbf{s}_1, & if\ |\mu\mathbf{s}_1 - \mathbf{z}| \le \mathbf{u}_{max} \\ \mathbf{z} - \mathbf{u}_{max}, & if\ (\mu\mathbf{s}_1 - \mathbf{z}) < -\mathbf{u}_{max} \end{cases} \tag{28}$$

Now consider the following Lyapunov function:

$$V_1 = \frac{1}{2}\mathbf{s}_1^T\mathbf{s}_1 \tag{29}$$

taking the derivative of (29), we obtain:

$$\dot{V}_1 = \mathbf{s}_1^T\dot{\mathbf{s}}_1 \tag{30}$$

by replacing $\mathbf{u}$ *with* $\mathrm{sat}(\mathbf{u})$ *in (13), we can rewrite (13) as:*

$$\dot{\mathbf{s}}_1 = \mathbf{f} + \mathbf{G}\,\mathrm{sat}(\mathbf{u}) + \mathbf{G}\mathbf{d} \tag{31}$$

Substituting (31) in (30) yields:

$$\dot{V}_1 = \mathbf{s}_1^T\big(\mathbf{f} + \mathbf{G}\,\mathrm{sat}(\mathbf{u}) + \mathbf{G}\mathbf{d}\big) \tag{32}$$

substituting the control law (16) in (32) yields:

$$\begin{aligned}\dot{V}_1 = \mathbf{s}_1^T\big(&-\mathbf{K}_1\,\mathrm{sig}(\mathbf{s}_1)^m - \mathbf{K}_2\,\mathrm{sig}(\mathbf{s}_1)^n \\ &- \mathbf{G}[\mathrm{sat}(\mu\mathbf{s}_1 - \mathbf{z}) + \mathbf{z}] + \mathbf{G}\mathbf{d}\big)\end{aligned} \tag{33}$$

with defining $\boldsymbol{\nu} = \mathbf{G}\mathbf{d}$*, we obtain:*

$$\begin{aligned}\dot{V}_1 = &-\mathbf{s}_1^T\mathbf{K}_1\,\mathrm{sig}(\mathbf{s}_1)^m - \mathbf{s}_1^T\mathbf{K}_2\,\mathrm{sig}(\mathbf{s}_1)^n \\ &- \mathbf{s}_1^T\mathbf{G}[\mathrm{sat}(\mu\mathbf{s}_1 - \mathbf{z}) + \mathbf{z}] + \mathbf{s}_1^T\boldsymbol{\nu}\end{aligned} \tag{34}$$

now considering (28) we can write:

$$\begin{aligned}\dot{V}_1 = &-\mathbf{s}_1^T\mathbf{K}_1\,\mathrm{sig}(\mathbf{s}_1)^m - \mathbf{s}_1^T\mathbf{K}_2\,\mathrm{sig}(\mathbf{s}_1)^n + \mathbf{s}_1^T\boldsymbol{\nu} \\ &- \begin{cases} \mathbf{s}_1^T\mathbf{G}(\mathbf{z} + \mathbf{u}_{max}), & if\ (\mu\mathbf{s}_1 - \mathbf{z}) > \mathbf{u}_{max} \\ \mu\mathbf{s}_1^T\mathbf{G}\mathbf{s}_1, & if\ |\mu\mathbf{s}_1 - \mathbf{z}| \le \mathbf{u}_{max} \\ \mathbf{s}_1^T\mathbf{G}(\mathbf{z} - \mathbf{u}_{max}), & if\ (\mu\mathbf{s}_1 - \mathbf{z}) < -\mathbf{u}_{max} \end{cases}\end{aligned} \tag{35}$$

considering (28) and the fact that $|\mathbf{z}| \le \mathbf{u}_{max}$*, one can obtain that* $\mathbf{z} + \mathbf{u}_{max} \ge \mathbf{0}$ *and* $\mathbf{z} - \mathbf{u}_{max} \le \mathbf{0}$*. Moreover, the terms* $\mu\mathbf{s}_1 - \mathbf{z} > \mathbf{u}_{max}$ *and* $\mu\mathbf{s}_1 - \mathbf{z} < -\mathbf{u}_{max}$*, result in* $\mathbf{s}_1 > \mathbf{0}$ *and* $\mathbf{s}_1 < \mathbf{0}$*, respectively. Since all the terms produce scalar values we have:*

$$\begin{aligned}\dot{V}_1 \le &-\|\mathbf{s}_1^T\mathbf{K}_1\,\mathrm{sig}(\mathbf{s}_1)^m\| - \|\mathbf{s}_1^T\mathbf{K}_2\,\mathrm{sig}(\mathbf{s}_1)^n\| + \|\mathbf{s}_1^T\boldsymbol{\nu}\| \\ &- \begin{cases} \|\mathbf{s}_1^T\mathbf{G}(\mathbf{z} + \mathbf{u}_{max})\|, & if\ (\mu\mathbf{s}_1 - \mathbf{z}) > \mathbf{u}_{max} \\ \|\mu\mathbf{s}_1^T\mathbf{G}\mathbf{s}_1\|, & if\ |\mu\mathbf{s}_1 - \mathbf{z}| \le \mathbf{u}_{max} \\ \|\mathbf{s}_1^T\mathbf{G}(\mathbf{z} - \mathbf{u}_{max})\|, & if\ (\mu\mathbf{s}_1 - \mathbf{z}) < -\mathbf{u}_{max} \end{cases}\end{aligned} \tag{36}$$

and therefore:

$$\begin{aligned}\dot{V}_1 \le &-\lambda_{min}(\mathbf{K}_1)\|\mathbf{s}_1\|^{m+1} - \lambda_{min}(\mathbf{K}_2)\|\mathbf{s}_1\|^{n+1} + \|\boldsymbol{\nu}\|\|\mathbf{s}_1\| \\ &- \begin{cases} \lambda_{min}(\mathbf{G})\|\mathbf{s}_1\|\|(\mathbf{z} + \mathbf{u}_{max})\|, & if\ (\mu\mathbf{s}_1 - \mathbf{z}) > \mathbf{u}_{max} \\ \mu\lambda_{min}(\mathbf{G})\|\mathbf{s}_1\|^2, & if\ |\mu\mathbf{s}_1 - \mathbf{z}| \le \mathbf{u}_{max} \\ \lambda_{min}(\mathbf{G})\|\mathbf{s}_1\|\|(\mathbf{z} - \mathbf{u}_{max})\|, & if\ (\mu\mathbf{s}_1 - \mathbf{z}) < -\mathbf{u}_{max} \end{cases}\end{aligned} \tag{37}$$

where $\lambda_{min}(\mathbf{K}_1) > 0$*,* $\lambda_{min}(\mathbf{K}_2) > 0$ *and* $\lambda_{min}(\mathbf{G}) > 0$ *are the minimum eigenvalues of* $\mathbf{K}_1$*,* $\mathbf{K}_2$ *and* $\mathbf{G}$*, respectively. Now since the last term of (37) is always negative, the inequality (37) can be reduced to:*

$$\begin{aligned}\dot{V}_1 &\le -\lambda_{min}(\mathbf{K}_1)\|\mathbf{s}_1\|^{m+1} - \lambda_{min}(\mathbf{K}_2)\|\mathbf{s}_1\|^{n+1} + \|\boldsymbol{\nu}\|\|\mathbf{s}_1\| \\ &\le -\|\mathbf{s}_1\|\left(\lambda_{min}(\mathbf{K}_1)\|\mathbf{s}_1\|^m + \lambda_{min}(\mathbf{K}_2)\|\mathbf{s}_1\|^n - \|\boldsymbol{\nu}\|\right)\end{aligned} \tag{38}$$

Now we can rewrite (38) in the following two forms [13]:

$$\dot{V}_1 \le -\|\mathbf{s}_1\|\Big(\big(\lambda_{min}(\mathbf{K}_1) - \frac{\|\boldsymbol{\nu}\|}{\|\mathbf{s}_1\|^m}\big)\|\mathbf{s}_1\|^m + \lambda_{min}(\mathbf{K}_2)\|\mathbf{s}_1\|^n\Big) \tag{39}$$

$$\dot{V}_1 \le -\|\mathbf{s}_1\|\Big(\lambda_{min}(\mathbf{K}_1)\|\mathbf{s}_1\|^m + \big(\lambda_{min}(\mathbf{K}_2) - \frac{\|\boldsymbol{\nu}\|}{\|\mathbf{s}_1\|^n}\big)\|\mathbf{s}_1\|^n\Big) \tag{40}$$

under the following conditions

$$\lambda_{min}(\mathbf{K}_1) - \frac{\|\boldsymbol{\nu}\|}{\|\mathbf{s}_1\|^m} > 0 \tag{41}$$

$$\lambda_{min}(\mathbf{K}_2) - \frac{\|\boldsymbol{\nu}\|}{\|\mathbf{s}_1\|^n} > 0 \tag{42}$$

and considering $\|\boldsymbol{\nu}\| \leq \|\mathbf{G}\|\|\mathbf{d}\| \leq \frac{1}{2}\bar{J}_{0max}d_{max}$*, we obtain that the sliding surface is bounded and it will reach the following small neighborhood of* $\mathbf{s}_1 = \mathbf{0}$ *as:*

$$\|\mathbf{s}_1\| \leq \Upsilon = \min\left\{\left(\frac{\bar{J}_{0max}d_{max}}{2\lambda_{min}(\mathbf{K}_1)}\right)^{\frac{1}{m}}, \left(\frac{\bar{J}_{0max}d_{max}}{2\lambda_{min}(\mathbf{K}_2)}\right)^{\frac{1}{n}}\right\} \tag{43}$$

Therefore, there exist a positive constant ϑ_1 *such that the inequality* $\vartheta_1 \geq \frac{1}{2}\Upsilon\bar{J}_{0max}d_{max}$ *holds. Thus, combining (29) with (38), we can obtain the following inequality:*

$$\dot{V}_1 \leq -2^a\lambda_{min}(\mathbf{K}_1)V_1^a - 2^b\lambda_{min}(\mathbf{K}_2)V_1^b + \vartheta_1 \tag{44}$$

where $0 < a = \frac{m+1}{2} < 1$ *and* $b = \frac{n+1}{2} > 1$*. Therefore, according to Lemma 2, the equilibrium of system (8) is practical fixed-time stable and the upper bound of the settling time is obtained as*

$$T_1 < T_{1max} \triangleq \frac{1}{2^a\lambda_{min}(\mathbf{K}_1)}\frac{1}{1-a} + \frac{1}{2^b\lambda_{min}(\mathbf{K}_2)}\frac{1}{b-1} \tag{45}$$

Therefore, system states will persistently converge to the pre-described sliding surface given in (8) in fixed time from any initial condition, even in the presence of unknown external disturbance and uncertainty.

Step 2 *Combining (43) with (8) yields*

$$s_{1i} = \dot{q}_{ei} + \Lambda_i\,\mathrm{D}^{\alpha-2}[\mathrm{sig}(q_{ei})^\lambda] + \Delta_{1i}\,\mathrm{D}^{\beta_1-2}[\mathrm{sig}(\dot{\eta}_{ei})^{\delta_1}] + \Delta_{2i}\,\mathrm{D}^{\beta_2-2}[\mathrm{sig}(\eta_{ei})^{\delta_2}], \quad |s_{1i}| \leq \Upsilon \tag{46}$$

where $i = 1, 2, 3$ *stands for the i-th degree of freedom (DoF) and elastic mode. Equation (46) can be transformed into the following three forms:*

$$\dot{q}_{ei} + \left(\Lambda_i - s_{1i}\big(\mathrm{D}^{\alpha-2}[\mathrm{sig}(q_{ei})^\lambda]\big)^{-1}\right)\mathrm{D}^{\alpha-2}[\mathrm{sig}(q_{ei})]^\lambda + \Delta_{1i}\,\mathrm{D}^{\beta_1-2}[\mathrm{sig}(\dot{\eta}_{ei})^{\delta_1}] + \Delta_{2i}\,\mathrm{D}^{\beta_2-2}[\mathrm{sig}(\eta_{ei})^{\delta_2}] = 0 \tag{47}$$

$$\dot{q}_{ei} + \Lambda_i\,\mathrm{D}^{\alpha-2}[\mathrm{sig}(q_{ei})^\lambda] + \left(\Delta_{1i} - s_{1i}\big(\mathrm{D}^{\beta_1-2}[\mathrm{sig}(\dot{\eta}_{ei})^{\delta_1}]\big)^{-1}\right)\mathrm{D}^{\beta_1-2}[\mathrm{sig}(\dot{\eta}_{ei})^{\delta_1}] + \Delta_{2i}\,\mathrm{D}^{\beta_2-2}[\mathrm{sig}(\eta_{ei})^{\delta_2}] = 0 \tag{48}$$

$$\dot{q}_{ei} + \Lambda_i\,\mathrm{D}^{\alpha-2}[\mathrm{sig}(q_{ei})^\lambda] + \Delta_{1i}\,\mathrm{D}^{\beta_1-2}[\mathrm{sig}(\dot{\eta}_{ei})^{\delta_1}] + \left(\Delta_{2i} - s_{1i}\big(\mathrm{D}^{\beta_2-2}[\mathrm{sig}(\eta_{ei})^{\delta_2}]\big)^{-1}\right)\mathrm{D}^{\beta_2-2}[\mathrm{sig}(\eta_{ei})^{\delta_2}] = 0 \tag{49}$$

Equation (47) will remain the proposed sliding surface given in (8) if the following inequality holds

$$\Lambda_i - s_{1i}\left(\mathrm{D}^{\alpha-2}[\mathrm{sig}(q_{ei})^\lambda]\right)^{-1} > 0 \tag{50}$$

Considering $|s_{1i}| \leq \Upsilon$*, the system states will continue converging to the proposed sliding surface until we have [13]:*

$$\left|\mathrm{D}^{\alpha-2}[\mathrm{sig}(q_{ei})^\lambda]\right| \leq \Lambda_i^{-1}\Upsilon \tag{51}$$

Taking Lemma 1 into consideration and choosing $p = \infty$*, we can obtain that*

$$ess\,sup\left|\mathrm{D}^{\alpha-2}[\mathrm{sig}(q_{ei})^\lambda]\right| \leq \kappa\; ess\,sup|q_{ei}|^\lambda = \kappa|q_{ei}|^\lambda_{max} \tag{52}$$

where $ess\,supf(x)$ *represents the essential maximum values of function* $f(x)$*. On the other hand, since we have* $\left|\mathrm{D}^{\alpha-2}[\mathrm{sig}(q_{ei})^\lambda]\right| \leq ess\,sup\left|\mathrm{D}^{\alpha-2}[\mathrm{sig}(q_{ei})^\lambda]\right|$*, we can write*

$$\left|\mathrm{D}^{\alpha-2}[\mathrm{sig}(q_{ei})^\lambda]\right| \leq \kappa|q_{ei}|^\lambda_{max} \tag{53}$$

Then, (53) can be transformed into following equality with a bounded time-varying factor $\sigma \geq 1$ *as*

$$\left|\mathrm{D}^{\alpha-2}[\mathrm{sig}(q_{ei})^\lambda]\right| = \sigma^{-1}\kappa|q_{ei}|^\lambda_{max} \tag{54}$$

with combining (51) and (54), we have

$$\sigma^{-1}\kappa|q_{ei}|^\lambda_{max} \leq \Lambda_i^{-1}\Upsilon \tag{55}$$

Therefore, the theoretical control errors will be bounded and can be given as

$$|q_{ei}| \leq |q_{ei}|_{max} \leq (\Lambda_i^{-1}\Upsilon\sigma\kappa^{-1})^{1/\lambda} \tag{56}$$

Applying the same analysis procedure to (48) and (49) yields

$$\left|\mathrm{D}^{\beta_1-2}[\mathrm{sig}(\dot{\eta}_{ei})^{\delta_1}]\right| \leq \Delta_{1i}^{-1}\Upsilon \tag{57}$$

$$\left|\mathrm{D}^{\beta_2-2}[\mathrm{sig}(\eta_{ei})^{\delta_2}]\right| \leq \Delta_{2i}^{-1}\Upsilon \tag{58}$$

and similarly we can calculate

$$|\dot{\eta}_{ei}| \leq |\dot{\eta}_{ei}|_{max} \leq (\Delta_{1i}^{-1}\Upsilon\sigma\kappa^{-1})^{1/\delta_1} \tag{59}$$

$$|\eta_{ei}| \leq |\eta_{ei}|_{max} \leq (\Delta_{2i}^{-1}\Upsilon\sigma\kappa^{-1})^{1/\delta_2} \tag{60}$$

Then, combining (51), (57) and (58) with (46), we have

$$|\dot{q}_{ei}| = |s_{1i}| + \left|\Lambda_i\,\mathrm{D}^{\alpha-2}[\mathrm{sig}(q_{ei})^\lambda]\right| + \left|\Delta_{1i}\,\mathrm{D}^{\beta_1-2}[\mathrm{sig}(\dot{\eta}_{ei})^{\delta_1}]\right| + \left|\Delta_{2i}\,\mathrm{D}^{\beta_2-2}[\mathrm{sig}(\eta_{ei})^{\delta_2}]\right| = 4\Upsilon \tag{61}$$

Therefore, stability of the control system is ensured and the system errors will be bounded by (56), (59), (60) and (61).

Combination of Step 1 and 2 completes the proof of Theorem 1.

Theorem 2 *For the spacecraft attitude control and modal vibration systems in (2), (3) and (4), with the proposed sliding surface in (22) and the designed active vibration controller in (25), if the hypothesis of Theorem 1 is satisfied and Assumptions 1, 2, 3 and 4 hold, the sliding surface of the active controller will reach a small neighborhood of origin within a fixed time, and all the corresponding signals of the closed-loop system will converge to a small neighborhood of origin in finite time in the presence of unknown external disturbance.*

Proof Applying the same analysis as Theorem 1 we obtain that the sliding surface (22) is bounded as

$$\|\mathbf{s}_2\| \leq \Phi = \min\left\{\left(\frac{\delta_{max}\|\dot{\boldsymbol{\omega}}\|}{\lambda_{min}(\mathbf{L}_1)}\right)^{\frac{1}{p}}, \left(\frac{\delta_{max}\|\dot{\boldsymbol{\omega}}\|}{\lambda_{min}(\mathbf{L}_2)}\right)^{\frac{1}{r}}\right\} \quad (62)$$

and therefore,

$$\dot{V}_2 \leq -2^c\lambda_{min}(\mathbf{L}_1)V_2^c - 2^d\lambda_{min}(\mathbf{L}_2)V_2^d + \vartheta_2 \quad (63)$$

where $0 < c = \frac{p+1}{2} < 1$, $d = \frac{r+1}{2} > 1$ and $\vartheta_2 \geq \delta_{max}\|\dot{\boldsymbol{\omega}}\|$. Therefore, according to Lemma 2, the equilibrium of system (22) is practical fixed-time stable and the upper bound of the settling time is obtained as

$$T_2 < T_{2max} \triangleq \frac{1}{2^c\lambda_{min}(\mathbf{L}_1)}\frac{1}{1-c} + \frac{1}{2^d\lambda_{min}(\mathbf{L}_2)}\frac{1}{d-1} \quad (64)$$

Furthermore, all the signals in $\mathbf{s}_2$ i.e. $\dot{\boldsymbol{\eta}}$ and $\boldsymbol{\eta}$, will remain bounded thereafter. When the attitude stabilization maneuver is complete, as $t \to \infty$, we have $\dot{\boldsymbol{\omega}} \to \mathbf{0}$. Therefore, the active controller can provide bounded vibration suppression as the maneuver completes, and it can provide full vibration suppression at the end of the stabilization maneuver once $\dot{\boldsymbol{\omega}} = \mathbf{0}$. Thus, the proof of Theorem 2 is completed.

Remark 6 Note that according to Theorem 1 and 2, one treats the question of spacecraft attitude control and appendages elastic mode stabilization separately where the coupling effect is treated as an external disturbance. Furthermore, Theorem 1 proves that the designed attitude controller can bring the modal displacement and velocity to a small neighborhood of zero, while, according to Theorem 2, once the active controller is in the loop, the modal displacement and velocity can reach zero in finite time.

In the next section, numerical simulation and comparison are given to verify the proposed attitude controller's success in conjunction with the active vibration control technique.

5 Numerical Simulation

In this section, the performance of the proposed controllers is evaluated using computer simulations in MATLAB software. The FONTSM and MFONTSM controllers' performance in passive/active vibration suppression of the flexible appendages are compared. Furthermore, the effectiveness of the proposed active controller (25) has been compared to the active MVFC controller ((81) in [2]) to study its superiority over the other methods.

5.1 Control Parameters

In order to get the best performance and robustness, the corresponding controller gains in (16) and (25) should be tuned appropriately. The controller gains selected by the trial-and-error method to reach the optimal response and performance of the closed-loop system are listed in Table 1.

Table 1: Controller Gains

$\boldsymbol{\Lambda} = \text{diag}(1.75, 0.75, 2) \times 0.15$	$\boldsymbol{\Gamma}_1 = \text{diag}(50, 50, 75)$
$\boldsymbol{\Delta}_1 = \text{diag}(0.15, 0.15, 0.15)$	$\boldsymbol{\Gamma}_2 = \text{diag}(100, 100, 100)$
$\boldsymbol{\Delta}_2 = \text{diag}(1, 0.05, 2)$	$\rho_1 = 0.75$
$\alpha = 0.70$	$\rho_2 = 0.65$
$\beta_1 = \beta_2 = 0.95$	$\gamma_1 = 0.58$
$\lambda = 0.45$	$\gamma_2 = 0.53$
$\delta_1 = 0.95$	$\mathbf{K}_1 = \mathbf{L}_1 = \text{diag}(0.1, 0.1, 0.1)$
$\delta_2 = 0.80$	$\mathbf{K}_2 = \mathbf{L}_2 = \text{diag}(0.01, 0.01, 0.01)$
$m = p = 0.52$	$\mu = 175$
$n = r = 3$	

5.2 Simulation Setup

System description of the flexible spacecraft for simulation studies are presented in Table 2 [6]. Assuming that

Table 2: System Description

Inertia Matrix	$\mathbf{J} = \begin{bmatrix} 420.8 & 3.6 & -4.2 \\ 3.6 & 410.6 & 9.4 \\ -4.2 & 9.4 & 690.7 \end{bmatrix}$ kg.m^2
Natural Frequency	$\boldsymbol{\Omega} = \text{diag}(0.379, 1.042, 1.331) \times 2\pi$ rad/s
Damping Ratio	$\boldsymbol{\zeta} = \text{diag}(0.005, 0.005, 0.005)$
Rigid-Flexible Coupling Matrix	$\boldsymbol{\delta} = \begin{bmatrix} 2.620 & 0.007 & -0.003 \\ -0.001 & 0.124 & -2.730 \\ -0.001 & 0.437 & -0.051 \end{bmatrix}$ kg$^{1/2}$m
Piezoelectric Coupling Matrix	$\boldsymbol{\delta}_p = \begin{bmatrix} 70.26 & -4.23 & 2.34 \\ 4.80 & 31.93 & 1.24 \\ -1.05 & 2.55 & 29.84 \end{bmatrix}$ kg$^{1/2}$m/(kVs^2)

the spacecraft is orbiting the planet at the altitude of 500 km, the total external disturbance is assumed as

$$\mathbf{d} = \begin{bmatrix} \cos(\omega_0 t) + 1 \\ \cos(\omega_0 t) + \sin(\omega_0 t) \\ \cos(\omega_0 t) + 1 \end{bmatrix} 4.5 \times 10^{-3}\,\text{N.m} \tag{65}$$

where $\omega_0 \approx 0.0011\,\text{rad/s}$ represents the orbital angular velocity [6]. Furthermore, to study the robustness of the controllers, 20% uncertainty on the inertia matrix and a zero damping matrix $\mathbf{C} = \mathbf{0}$ is considered in all the simulations. The actuators' saturation bound is set as $u_{max} = 10\,\text{N.m}$, and since we aim to perform attitude stabilization and vibration suppression, we have $\boldsymbol{\omega}_d = \dot{\boldsymbol{\omega}}_d = \boldsymbol{\eta}_d = \dot{\boldsymbol{\eta}}_d = [0,\, 0,\, 0]^T$.

5.3 Simulation Results

The simulation results of the FONTSM controller ((20) where $\boldsymbol{\Delta}_1 = \boldsymbol{\Delta}_2 = \mathbf{0}$) and MFONTSM controller (20) with active OFF, active MVFC ((81) in [2]) and active FONTSM (25) are shown in Fig. 2 and 3, respectively. For the proposed controllers, all the control gains are presented in Table 1, and for the MVFC controller, everything is as in [2], except the gain $\mathbf{F} = \text{diag}(10, 10, 10)$, which is chosen for better performance.

It can be observed from Fig. 2 that there is a negligible difference for the FONTSM controller once the active controller is OFF with active MVFC and active FONTSM; in Euler angles, attitude quaternion, angular velocity, and the sliding surface plots as all the graphs overlap. The upper bound of the settling time for the attitude FONTSM controller can be calculated using (45) and Table 1 as $T_{1max} = 49.6040\,\text{s}$, independent of the initial conditions, therefore all the signals in the sliding surface should be settled before $T_{1max} = 49.6040\,\text{s}$ is reached. The tracking errors in Euler angles for all controllers are less than 0.02 degree when $t \geq T_{1max}$. Predictably, the main difference can be seen in modal displacement and velocity plots. The attitude FONTSM controller cannot provide any vibration suppression, and therefore, since there is no damping matrix, the vibration amplitude increases over time. However, once the active controllers are in the loop, modal vibrations are properly controlled and neutralized. Furthermore, comparing the performance of the active MVFC with active FONTSM, a noticeable difference can be observed in the settling time, maximum overshoot, and the steady-state error of appendages modal displacement and velocity. The upper bound of the settling time for the active FONTSM controller can be calculated using (64) and Table 1 as $T_{2max} = 51.9931\,\text{s}$, independent of the modal initial conditions. It can be observed from analyzing the plots that the modal displacement error for the active MVFC and active FONTSM are under 5×10^{-6} and 5×10^{-9}, respectively, when $t \geq T_{2max}$.

Furthermore, it can be observed in Fig. 3 that there is a slight difference for the MFONTSM controller once the active controller is OFF with active MVFC and active FONTSM; in Euler angles, attitude quaternion, angular velocity, and the sliding surface plots. Comparing the modal displacement and velocity plots from Fig. 2 and 3, it can be seen that despite the FONTSM controller, the MFONTSM controller can provide passive vibration suppression once the active controller is OFF. The upper bound of the settling time for the attitude MFONTSM controller is $T_{1max} = 49.6040\,\text{s}$, and the tracking errors in Euler angles for all controllers are less than 0.02 degree when $t \geq T_{1max}$ as before. However, despite the FONTSM controller, since the modal displacement and velocity exist in the modified sliding surface, both modal displacement and velocity are settled before $T_{1max} = 49.6040\,\text{s}$ is reached. The upper bound of the active FONTSM controller's settling time is again calculated as $T_{2max} = 51.9931\,\text{s}$. It can be observed from analyzing the plots that the modal displacement error for the MFONTSM controller with active OFF, active MVFC, and active FONTSM are under 5×10^{-5}, 5×10^{-7}, and 5×10^{-10}, respectively, when $t \geq T_{2max}$. Comparing the control torque plots in Fig. 2 and 3 shows that the passive MFONTSM controller experiences more chattering than the FONTSM controller at the beginning of the maneuver, which is an expected consequence of the sliding surface modification. It can also be deduced from the piezoelectric voltage plots that the active FONTSM uses a bit more voltage comparing to the active MVFC controller.

6 Conclusion

This paper studies the problem of flexible spacecraft attitude control and appendages vibration suppression by introducing a new fractional-order nonsingular terminal sliding mode (FONTSM) controller. A modified FONTSM (MFONTSM) controller is introduced by designing a novel multi-purpose sliding surface that can perform passive vibration suppression. Furthermore, an active FONTSM controller is proposed separately for active vibration suppression using piezoelectric actuators. The total practical fixed-time stability of the closed-loop system and the boundedness of all the subsequent error signals have been analyzed and proved using the Lyapunov theorem. The proposed control scheme's performance has been studied through numerical simulations. It is observed that the proposed control scheme

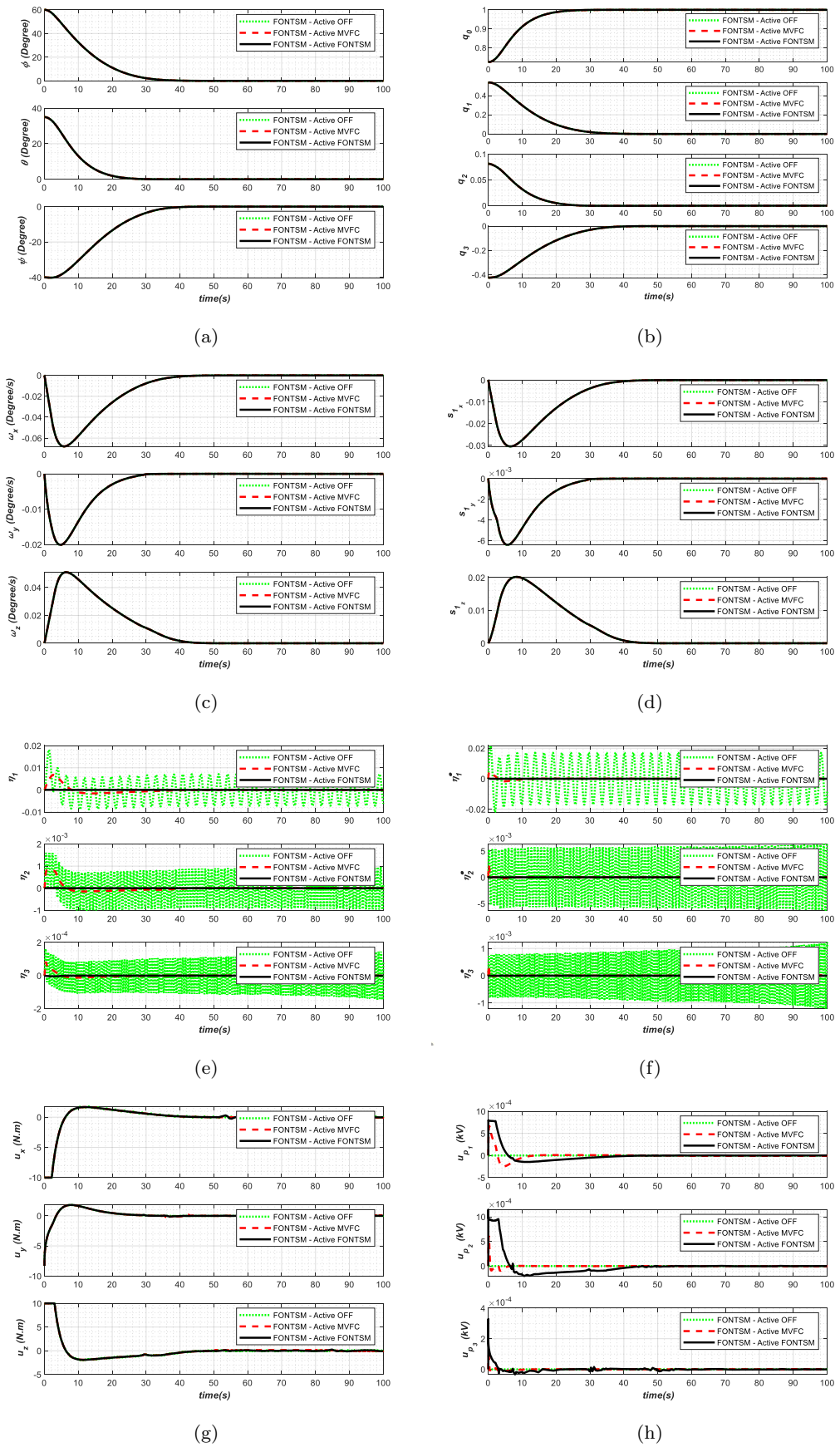

Fig. 2: Simulation responses of the FONTSM controller under external disturbance and uncertainty. (a) Euler angles (ϕ, θ, ψ). (b) Attitude quaternion (q_0, q_1, q_2, q_3). (c) Angular velocity $(\omega_x, \omega_y, \omega_z)$. (d) Sliding surface $(s_{1_x}, s_{1_y}, s_{1_z})$. (e) Modal displacement (η_1, η_2, η_3). (f) Modal velocity $(\dot{\eta}_1, \dot{\eta}_2, \dot{\eta}_3)$. (g) Control torque (u_x, u_y, u_z). (h) Piezoelectric voltage $(u_{p_1}, u_{p_2}, u_{p_3})$. (Figures are zoomable)

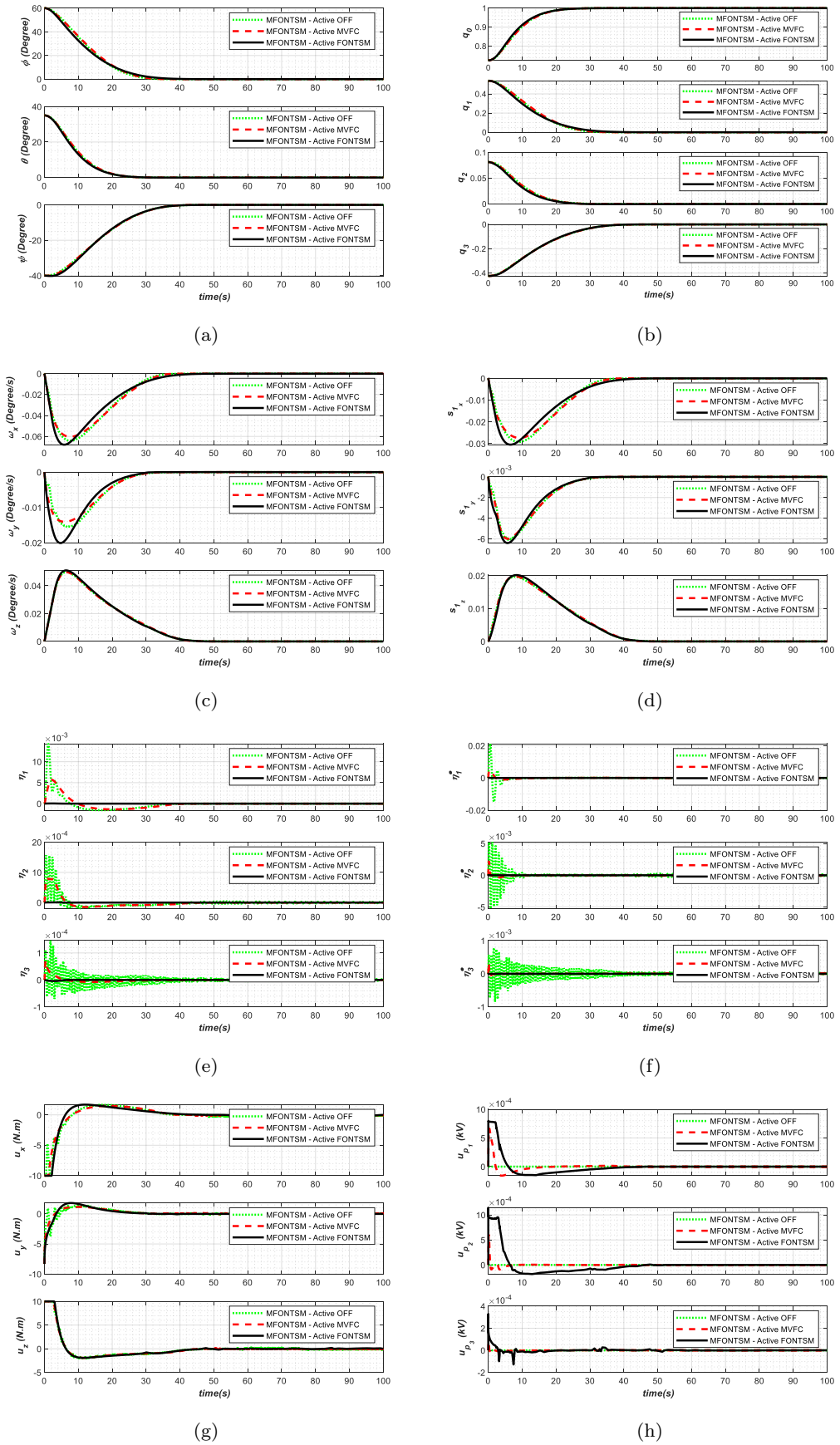

Fig. 3: Simulation responses of the MFONTSM controller under external disturbance and uncertainty. (a) Euler angles (ϕ, θ, ψ). (b) Attitude quaternion (q_0, q_1, q_2, q_3). (c) Angular velocity $(\omega_x, \omega_y, \omega_z)$. (d) Sliding surface $(s_{1_x}, s_{1_y}, s_{1_z})$. (e) Modal displacement (η_1, η_2, η_3). (f) Modal velocity $(\dot{\eta}_1, \dot{\eta}_2, \dot{\eta}_3)$. (g) Control torque (u_x, u_y, u_z). (h) Piezoelectric voltage $(u_{p_1}, u_{p_2}, u_{p_3})$. (Figures are zoomable)

can provide fast convergence with short settling time and small overshoot/undershoot with passive vibration suppression ability. Furthermore, the proposed controllers' effectiveness is studied under uncertainty, unexpected external disturbance, and the damping matrix's absence. It is observed that the proposed active controller can provide faster convergence with far less steady-state error compared to previous methods.

Conflict of Interest

The authors declare that they have no conflict of interest.

References

1. Shijie Xu, Naigang Cui, Youhua Fan, and Yingzi Guan. Flexible satellite attitude maneuver via adaptive sliding mode control and active vibration suppression. *AIAA Journal*, 56(10):4205–4212, 2018.
2. Chengbao Zhou and Di Zhou. Robust dynamic surface sliding mode control for attitude tracking of flexible spacecraft with an extended state observer. *Proceedings of the Institution of Mechanical Engineers, Part G: Journal of Aerospace Engineering*, 231(3):533–547, 2017.
3. Qinglei Hu. Sliding mode maneuvering control and active vibration damping of three-axis stabilized flexible spacecraft with actuator dynamics. *Nonlinear Dynamics*, 52(3):227–248, 2008.
4. Qiufan Yuan, Yanfang Liu, and Naiming Qi. Active vibration suppression for maneuvering spacecraft with high flexible appendages. *Acta Astronautica*, 139:512–520, 2017.
5. Naiming Qi, Qiufan Yuan, Yanfang Liu, Mingying Huo, and Shilei Cao. Consensus vibration control for large flexible structures of spacecraft with modified positive position feedback control. *IEEE Transactions on Control Systems Technology*, 27(4):1712–1719, 2018.
6. Chao Zhang, Guangfu Ma, Yanchao Sun, and Chuanjiang Li. Prescribed performance adaptive attitude tracking control for flexible spacecraft with active vibration suppression. *Nonlinear Dynamics*, 96(3):1909–1926, 2019.
7. Yuliang Bai, James D Biggs, Franco Bernelli Zazzera, and Naigang Cui. Adaptive attitude tracking with active uncertainty rejection. *Journal of Guidance, Control, and Dynamics*, 41(2):550–558, 2018.
8. Qinglei Hu, Xiaodong Shao, Youmin Zhang, and Lei Guo. Nussbaum-type function–based attitude control of spacecraft with actuator saturation. *International Journal of Robust and Nonlinear Control*, 28(8):2927–2949, 2018.
9. Bo Li, Qinglei Hu, and Guangfu Ma. Extended state observer based robust attitude control of spacecraft with input saturation. *Aerospace Science and Technology*, 50:173–182, 2016.
10. Boyan Jiang, Qinglei Hu, and Michael I Friswell. Fixed-time attitude control for rigid spacecraft with actuator saturation and faults. *IEEE Transactions on Control Systems Technology*, 24(5):1892–1898, 2016.
11. Seyed Majid Esmailzadeh and Mehdi Golestani. Comment on "fixed-time attitude control for rigid spacecraft with actuator saturation and faults". *IEEE Transactions on Control Systems Technology*, 27(4):1846–1846, 2018.
12. An-Min Zou and Krishna Dev Kumar. Finite-time attitude control for rigid spacecraft subject to actuator saturation. *Nonlinear Dynamics*, 96(2):1017–1035, 2019.
13. Yaoyao Wang, Linyi Gu, Yihong Xu, and Xiaoxu Cao. Practical tracking control of robot manipulators with continuous fractional-order nonsingular terminal sliding mode. *IEEE Transactions on Industrial Electronics*, 63(10):6194–6204, 2016.
14. Yaoyao Wang, Binbin Li, Fei Yan, and Bai Chen. Practical adaptive fractional-order nonsingular terminal sliding mode control for a cable-driven manipulator. *International Journal of Robust and Nonlinear Control*, 29(5):1396–1417, 2019.
15. Guanghui Sun, Zhiqiang Ma, and Jinyong Yu. Discrete-time fractional order terminal sliding mode tracking control for linear motor. *IEEE Transactions on Industrial Electronics*, 65(4):3386–3394, 2017.
16. Andrey Polyakov. Nonlinear feedback design for fixed-time stabilization of linear control systems. *IEEE Transactions on Automatic Control*, 57(8):2106–2110, 2011.
17. Zongyu Zuo, Qing-Long Han, Boda Ning, Xiaohua Ge, and Xian-Ming Zhang. An overview of recent advances in fixed-time cooperative control of multiagent systems. *IEEE Transactions on Industrial Informatics*, 14(6):2322–2334, 2018.
18. Igor Podlubny. *Fractional differential equations: an introduction to fractional derivatives, fractional differential equations, to methods of their solution and some of their applications*, volume 198. Elsevier, 1998.
19. Kai Diethelm. *The analysis of fractional differential equations: An application-oriented exposition using differential operators of Caputo type*. Springer Science & Business Media, 2010.
20. Chun Yin, YangQuan Chen, and Shou-ming Zhong. Fractional-order sliding mode based extremum seeking control of a class of nonlinear systems. *Automatica*, 50(12):3173–3181, 2014.
21. Qiang Chen, Shuzong Xie, Mingxuan Sun, and Xiongxiong He. Adaptive nonsingular fixed-time attitude stabilization of uncertain spacecraft. *IEEE Transactions on Aerospace and Electronic Systems*, 54(6):2937–2950, 2018.
22. Lubomir Dorcak. Numerical models for the simulation of the fractional-order control systems. *arXiv preprint math/0204108*, 2002.
23. Zhuoyue Song, Chao Duan, Housheng Su, and Jinchang Hu. Full-order sliding mode control for finite-time attitude tracking of rigid spacecraft. *IET Control Theory & Applications*, 12(8):1086–1094, 2018.
24. Qinglei Hu. Robust adaptive sliding mode attitude maneuvering and vibration damping of three-axis-stabilized flexible spacecraft with actuator saturation limits. *Nonlinear Dynamics*, 55(4):301, 2009.
25. Shidong Xu, Guanghui Sun, Zhiqiang Ma, and Xiaolei Li. Fractional-order fuzzy sliding mode control for the deployment of tethered satellite system under input saturation. *IEEE Transactions on Aerospace and Electronic Systems*, 2018.
26. Xiuyun Zhang, Qun Zong, Liqian Dou, Bailing Tian, and Wenjing Liu. Finite-time attitude maneuvering and vibration suppression of flexible spacecraft. *Journal of the Franklin Institute*, 2019.

Figures

Figure 1

Schematic of the flexible spacecraft

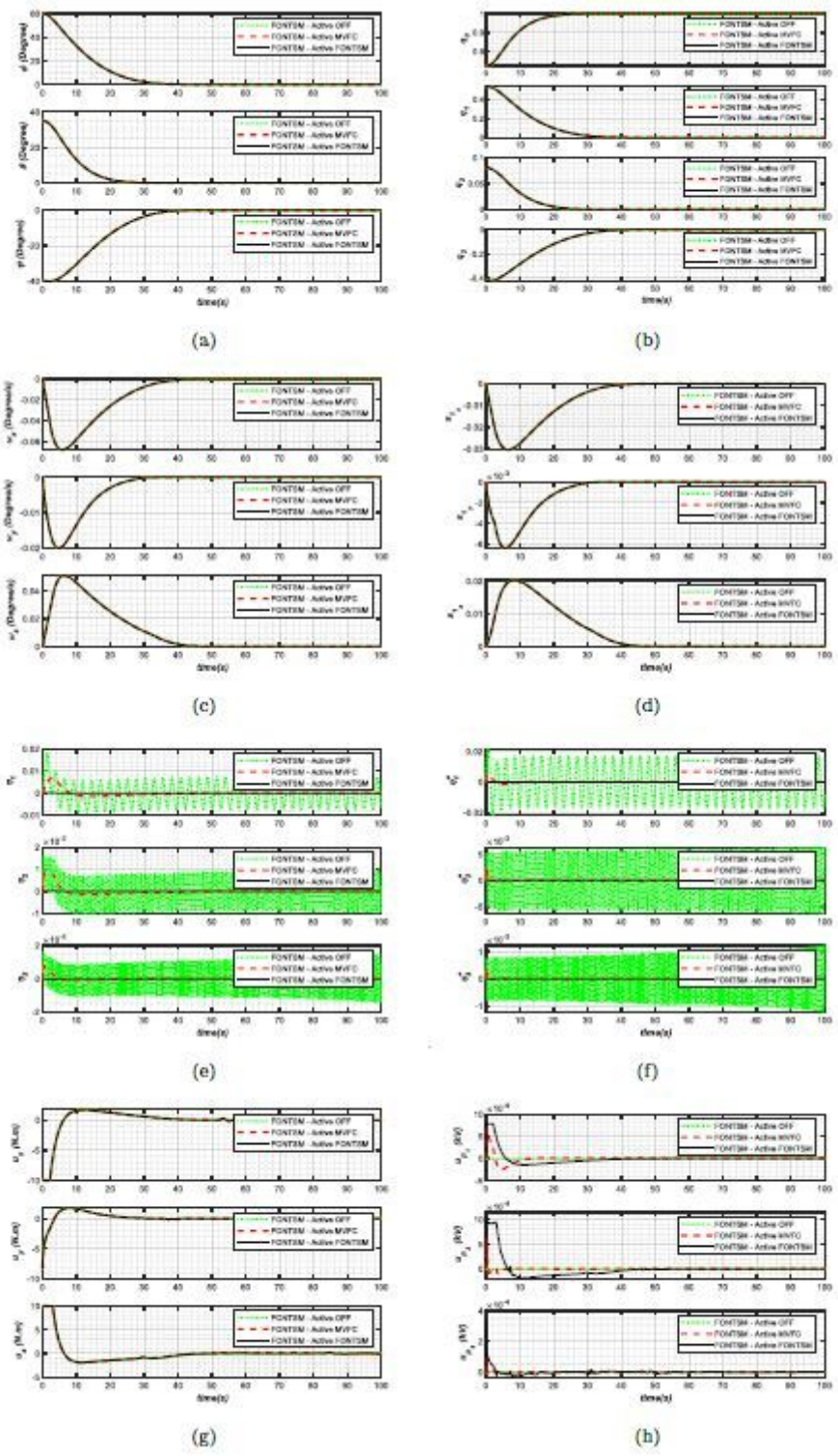

Figure 2

"Please see the Manuscript PDF file for the complete figure caption".

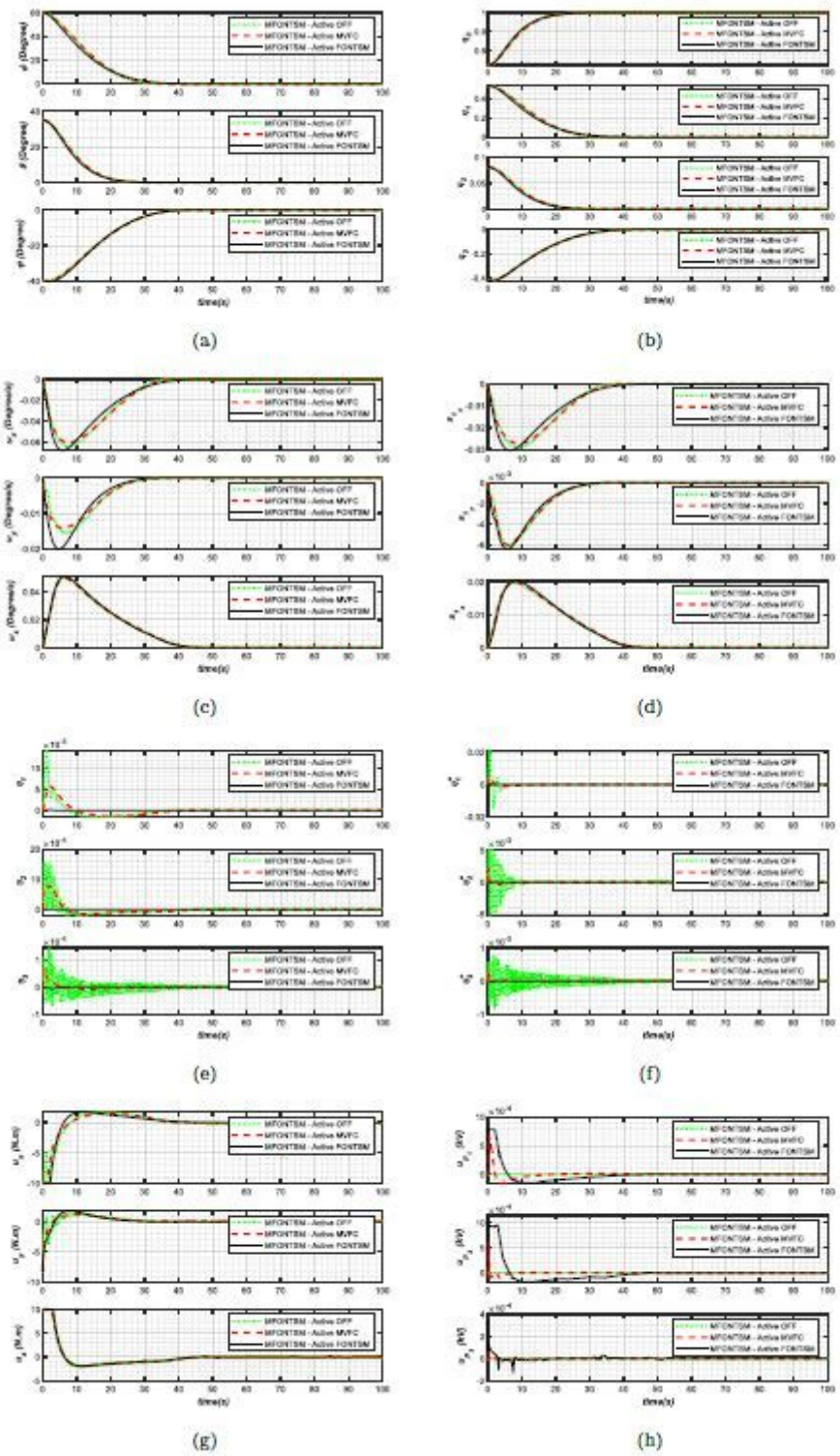

Figure 3

"Please see the Manuscript PDF file for the complete figure caption".